

## Antikaons in nuclei and dense nuclear matter

A. Ramos<sup>a</sup>, S. Hirenzaki<sup>b</sup>, S.S. Kamalov<sup>c</sup>, T.T.S. Kuo<sup>d</sup>, Y. Okumura<sup>b</sup>, E. Oset<sup>e</sup>,  
A. Polls<sup>a</sup>, H. Toki<sup>f</sup> and L. Tolós<sup>a</sup>

<sup>a</sup> Departament d'Estructura i Constituents de la Matèria, Universitat de Barcelona,  
Diagonal 647, 08028 Barcelona, Spain

<sup>b</sup>Department of Physics, Nara Women's University, Nara 630-8506, Japan

<sup>c</sup>Laboratory of Theoretical Physics, JINR Dubna, 141980 Moscow region, Russia

<sup>d</sup>Department of Physics and Astronomy, State University of New York, Stony Brook,  
NY 11794, USA

<sup>e</sup> Departamento de Física Teórica and IFIC, Institutos de Investigación de Paterna,  
Aptdo. Correos 22085, 46071 Valencia, Spain

<sup>f</sup>Research Center for Nuclear Physics (RCNP), Osaka University, Ibaraki, Osaka  
567-0047, Japan

We present recent progress on the properties of antikaons in nuclei and dense nuclear matter as obtained from two  $\bar{K}N$  interaction models: one based on the lowest-order meson-baryon chiral lagrangian and the other derived from a meson-exchange picture.

### 1. Introduction

Understanding the properties of kaons and antikaons in the nuclear medium is of especial relevance in the analysis of data from heavy-ion collisions, as well as in the physics of neutron stars interiors. In the latter case, a condensed phase of  $K^-$  mesons might appear if they develop enough attraction in the medium, such that it becomes more favorable to neutralize the positive proton charge with antikaons rather than with electrons [1–7]. Analysis of kaonic atom data, sensitive to low densities, favor a strongly attractive  $K^-$  nucleus interaction [8,9], although recently weaker potentials have also been shown to describe the data appropriately [10,11]. Information on the higher density regime can be inferred from the analysis of heavy-ion collisions data. For instance, the enhancement of the  $K^-$  yield measured recently at GSI [12] can be explained by a strong attraction in the medium for the  $K^-$  [13,14], although an alternative mechanism, based on the in-medium enhanced  $\pi\Sigma \rightarrow K^-p$  reaction, has also been suggested [15].

Although all experimental indications point at an attractive antikaon potential in the nuclear medium, the size of this attraction has not really been well constrained by the data. It is therefore interesting to explore what the theoretical models predict. A traditional perspective is that of mean field approaches, built within the modern framework

of chiral lagrangians [14,16,17] or based on the relativistic Walecka model [18]. However, an especially useful point of view is that provided by microscopic models [19–24], since they establish a bridge between the properties of the  $\bar{K}N$  interaction in the medium and those in free space. This is the approach followed in the present contribution, where we will focus on the results obtained with two different  $\bar{K}N$  interactions: one is taken from the modern chiral meson-baryon lagrangian in  $S$ -wave [25], and the other is the meson-exchange model of the Jülich group [26].

## 2. $\bar{K}N$ interaction in free space

The dynamics of  $\bar{K}N$  scattering is dominated by the presence of an isospin zero  $S$ -wave resonance, the  $\Lambda(1405)$ . In potential models the  $\bar{K}N$  scattering observables ( $\bar{K} = K^-$  or  $\bar{K}^0$ ) are derived from the scattering amplitude, obtained from the Bethe-Salpeter equation

$$T_{ij} = V_{ij} + V_{il}G_lT_{lj} , \quad (1)$$

where the diagonal loop operator  $G_l$  stands for the intermediate meson-baryon ( $MB$ ) propagator and  $V$  is a suitable  $MB \rightarrow M'B'$  transition potential.

A connection with the chiral lagrangian was established in ref. [27], where the properties of the strangeness  $S = -1$  meson-baryon sector were studied in a potential model that, in Born approximation, had the same  $S$ -wave scattering length as the chiral lagrangian, including both the lowest order and the momentum dependent  $p^2$  terms. Fitting five parameters, the scattering observables were reproduced and the  $\Lambda(1405)$  resonance was generated dynamically from a coupled-channels Lippmann-Schwinger equation which included the meson-baryon states opened at the  $\bar{K}N$  threshold. In ref. [25] it was shown that the data could be reproduced using only the lowest order lagrangian and one parameter, the cut-off used to regularize the loop  $G_l$ . The value of the cut-off,  $q_{\max} = 630$  MeV, was chosen to reproduce the  $K^-p$  scattering branching ratios at threshold. The essential difference with respect to ref. [27] was the inclusion in ref. [25] of all ten meson-baryon states ( $K^-p$ ,  $\bar{K}^0n$ ,  $\pi^0\Lambda$ ,  $\pi^+\Sigma^-$ ,  $\pi^0\Sigma^0$ ,  $\pi^-\Sigma^+$ ,  $\eta\Lambda$ ,  $\eta\Sigma^0$ ,  $K^+\Xi^-$  and  $K^0\Xi^0$ ) that can be generated from the octet of pseudoscalar mesons and the octet of ground-state baryons, the  $\eta\Lambda$  state being the most relevant of the new included ones. The success of this method is analogous to that obtained in the meson-meson sector [28], an explanation of which is found by applying the Inverse Amplitude Method in coupled channels taking the lowest and next-to-lowest order meson-meson lagrangians [29]. A more recent work corroborates the success of the lowest order meson-baryon lagrangian in reproducing the  $\bar{K}N$  scattering observables from the point of subtracted dispersion relations [30].

We will also explore the antikaon properties as obtained from the  $\bar{K}N$  Jülich interaction [26], which is based on a meson-exchange picture. Most of the parameters were taken from their  $KN$  potential in the strangeness  $S = 1$  sector and the few free ones left were adjusted to reproduce the  $K^-p$  elastic and inelastic cross section data at low energies. The advantage of this interaction is that it contains all partial waves and allows for an investigation of their effect on the antikaon potential at the high momenta explored by heavy-ion collisions.

Although both  $\bar{K}N$  interactions describe reasonably well the low energy  $K^-p$  elastic and inelastic cross sections, some of the scattering observables at threshold, summarized

in Table 1, are not well reproduced. Clearly, some improvements can still be made for the Jülich  $\bar{K}N$  interaction since the branching ratios were not used for adjusting the parameters of the model.

Table 1  
 $\bar{K}N$  scattering observables at threshold

	Chiral [25]	Jülich [26]	EXP [31–33]
$\frac{\Gamma(K^-p \rightarrow \pi^+\Sigma^-)}{\Gamma(K^-p \rightarrow \pi^-\Sigma^+)}$	2.32	5.78	$2.36 \pm 0.04$
$\frac{\Gamma(K^-p \rightarrow \text{charged particles})}{\Gamma(K^-p \rightarrow \text{all})}$	0.627	0.600	$0.664 \pm 0.011$
$\frac{\Gamma(K^-p \rightarrow \pi^0\Lambda)}{\Gamma(K^-p \rightarrow \text{neutral states})}$	0.213	0.447	$0.189 \pm 0.015$
$a^{I=0}$ (fm)	$-1.93 + i 1.68$	$-1.71 + i 1.28$	$-1.70 + i 0.68$
$a^{I=1}$ (fm)	$0.52 + i 0.51$	$1.07 + i 0.71$	$0.37 + i 0.60$

### 3. $K^-$ deuteron scattering

The amplitudes of the chiral model were used in ref. [34] to study  $K^-$  scattering off the deuteron, the lightest nucleus. It is well known that the impulse approximation fails in describing the  $K^-$  scattering length and that more sophisticated approaches based on the solution of the Fadeev equations are required [35–37]. In ref. [34] the coupled-channels Fadeev equations were solved in the so-called fixed center approximation (FCA) including the  $K^-pn$  and the charge exchange  $\bar{K}^0nn$  channels, since those involving pions were found to give a small contribution. The resulting  $K^-$  deuteron scattering length is

$$A_{Kd} = \frac{M_d}{m_K + M_d} \int d\mathbf{r} |\varphi_d(\mathbf{r})|^2 \hat{A}_{Kd}(r), \quad (2)$$

with

$$\hat{A}_{Kd}(r) = \frac{\tilde{a}_p + \tilde{a}_n + (2\tilde{a}_p\tilde{a}_n - b_x^2)/r - 2b_x^2\tilde{a}_n/r^2}{1 - \tilde{a}_p\tilde{a}_n/r^2 + b_x^2\tilde{a}_n/r^3}, \quad (3)$$

where  $\tilde{a} = a(1 + m_K/m_N)$ , and  $b_x = \tilde{a}_x/\sqrt{1 + \tilde{a}_n^0/r}$  is the charge exchange amplitude renormalized due to the  $\bar{K}^0n$  rescattering. Expanding Eq. (3) to different orders in  $(1/r)$  gives rise to the different approximations, such as the impulse approximation (IA) (order zero) or the IA plus double rescattering (first order). In Table 2 we collect the results of ref. [34] obtained from the chiral elementary  $\bar{K}N$  amplitudes calculated using the physical basis or the isospin basis at an energy  $W = m_K + m_N = 1431.6$  MeV.

We first observe that the results from the lowest orders differ appreciably from those obtained by summing the full Fadeev series in the FCA given by Eqs. (2), (3). Secondly, the  $K^-$  deuteron scattering length obtained from scattering amplitudes that rely on isospin symmetry differ appreciably from that obtained within the physical basis. Finally, the result  $A_{Kd} = -1.62 + i 1.91$  fm differs from previous multichannel Fadeev

Table 2  
 $K^-$ -deuteron scattering length (in fm) calculated using different approximations

	Physical basis	Isospin basis
IA	$-0.260 + i 1.872$	$-0.318 + i 2.013$
IA + double resc.	$-2.735 + i 2.895$	$-3.168 + i 3.717$
$A_{Kd}$ (only el.resc.)	$-1.161 + i 1.336$	$-1.255 + i 1.518$
$A_{Kd}$ (total)	$-1.615 + i 1.909$	$-1.909 + i 2.455$

approaches,  $A_{Kd} = -1.47 + i 1.08$  fm [36] and  $A_{Kd} = -1.34 + i 1.04$  fm [37], especially for the imaginary part. As observed in ref. [34], this is mainly due to the different elementary amplitudes used in the different works. In fact, taking the amplitudes of ref. [37] and using isospin symmetry, which leads to a particularly small imaginary part for the charge exchange  $K^-p \rightarrow \bar{K}^0n$  amplitude, one obtains the FCA result  $A_{Kd} = -1.54 + i 1.29$  fm, very close to that quoted in ref. [37]. The studies in ref. [38], together with the analysis performed in ref. [34], show that one can associate the remaining differences to the FCA which overestimates the full Fadeev calculation by about 15%.

Although the results described here show that it is not simple to extract the elementary scattering amplitudes from the deuteron data, it can nevertheless be expected that the experimental results from the DEAR experiment at Frascati will introduce a further check of consistency between elementary amplitudes and should bring some light into issues like chiral symmetry and partial isospin breakup.

#### 4. $\bar{K}$ in nuclear matter

One source of medium modification of the  $\bar{K}N$  amplitude is that induced by Pauli-blocking [20,21] which effectively shifts the intermediate  $\bar{K}N$  states, and in turn the  $\Lambda(1405)$  resonance, to higher energies. Due to the strong energy dependence, this shift changes the  $\bar{K}N$  amplitude around threshold from being repulsive in free space to being attractive in the medium. The  $\bar{K}$  meson thus develops an attractive potential which, when incorporated in the equation determining the in-medium  $\bar{K}N$  amplitude, compensates the repulsive effect of Pauli blocking. When these effects are considered self-consistently, it is observed that the position of the  $\Lambda(1405)$  remains unchanged [22]. Since the  $\pi\Sigma$  states have a strong influence in the dynamics of  $\bar{K}N$  scattering, the dressing of pions was also considered in the study of ref. [23], together with mean-field potentials for the baryons participating in the coupled-channels problem. These medium effects are incorporated by replacing the free baryon and meson propagators by dressed ones in the meson-baryon loop-function which then reads

$$\begin{aligned}
 G(P^0, \vec{P}, \rho) &= \int_{|\vec{q}| < q_{\max}} \frac{d^3q}{(2\pi)^3} \frac{M}{E(-\vec{q})} \int_0^\infty d\omega S(\omega, \vec{q}, \rho) \\
 &\times \left\{ \frac{1 - n(\vec{q}_{\text{lab}})}{\sqrt{s} - \omega - E(-\vec{q}) + i\epsilon} + \frac{n(\vec{q}_{\text{lab}})}{\sqrt{s} + \omega - E(-\vec{q}) - i\epsilon} \right\}, \quad (4)
 \end{aligned}$$

where  $(P^0, \vec{P})$  is the total four-momentum in the lab frame,  $n(\vec{q}_{\text{lab}})$  is the nucleon occupation probability, and  $S(\omega, \vec{q}, \rho) = -\text{Im}D(\omega, \vec{q}, \rho)/\pi$  is the  $\bar{K}$  spectral density, which in free space reduces to  $\delta(\omega - \omega(\vec{q}))/2\omega(\vec{q})$ . The in-medium antikaon propagator,  $D(\omega, \vec{q}, \rho)$ , is determined from the antikaon self-energy,  $\Pi_K(\omega, \vec{q}, \rho)$ , which is obtained by summing the in-medium  $\bar{K}N$  interaction,  $T_{\text{eff}}(P^0, \vec{P}, \rho)$ , over the nucleons in the Fermi sea

$$\Pi_K(q^0, \vec{q}, \rho) = 2 \sum_{N=n,p} \int \frac{d^3p}{(2\pi)^3} n(\vec{p}) T_{\text{eff}}(q^0 + E(\vec{p}), \vec{q} + \vec{p}, \rho). \quad (5)$$

Note that a self-consistent approach is required since one calculates the  $\bar{K}$  self-energy from the effective interaction  $T_{\text{eff}}$  which uses  $\bar{K}$  propagators which themselves include the self-energy being calculated.

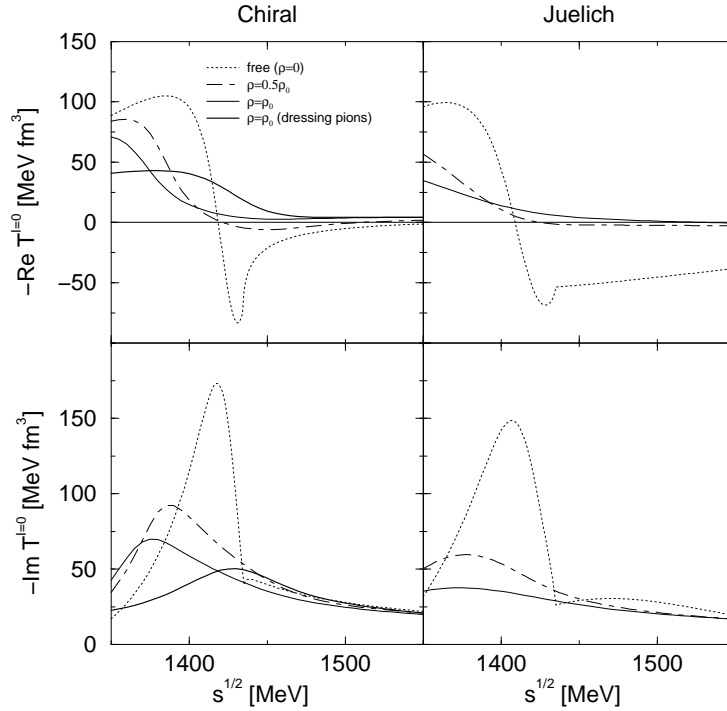


Figure 1. Real and imaginary parts of the  $I = 0$   $\bar{K}N$  scattering amplitude as functions of  $\sqrt{s}$  for  $|\vec{p}_K + \vec{p}_N| = 0$  and several densities (from [23] and [24]).

The free  $\bar{K}N$  amplitude in the  $I = 0$ ,  $L = 0$  channel is shown in Fig. 1, where it is compared with the in-medium one at two nuclear densities,  $\rho = \rho_0 = 0.17 \text{ fm}^{-3}$  and  $\rho = 0.5\rho_0$ . Results are shown for two different calculations, that of ref. [23], based on the chiral lagrangian model [25], and that of ref. [24], based on the meson-exchange  $\bar{K}N$  interaction [26]. We observe that the medium modified amplitudes show the same qualitative trends. Note also how the real part of the amplitude (upper panels) at the

$K^-p$  threshold ( $\sqrt{s} = 1433$  MeV) is repulsive in free space and attractive in the medium. The thick solid line on the left panels show the additional effect on the  $\bar{K}N$  amplitude of dressing the pions in the intermediate states [23].

Most of the available models study the in-medium  $\bar{K}N$  amplitude in  $S$ -wave. However, if one aims at extracting the properties of antikaons through the analysis of heavy-ion collisions, one must keep in mind that they are created at a finite momentum of around 250 – 500 MeV/c, hence the effect of higher partial waves might be relevant. The meson-exchange  $\bar{K}N$  potential of the Jülich group [26] is given in partial waves and allows a straightforward analysis of the importance of the  $L > 0$  components. From the chiral perspective, the  $P$ -wave amplitudes up to the next-to-leading order  $\bar{K}N$  chiral lagrangian have been identified and the parameters have been fitted to reproduce a large amount of low energy data [39]. However, a nuclear medium application of this model is not available yet.

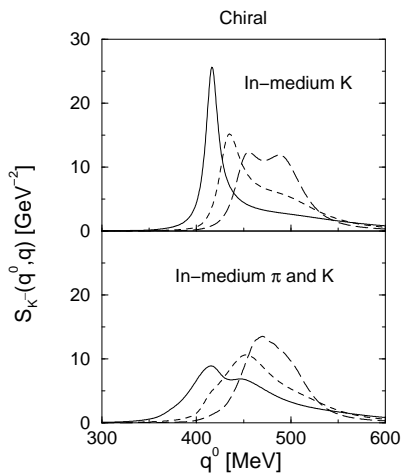


Figure 2.  $K^-$  spectral density for zero momentum from the chiral model of ref. [23]

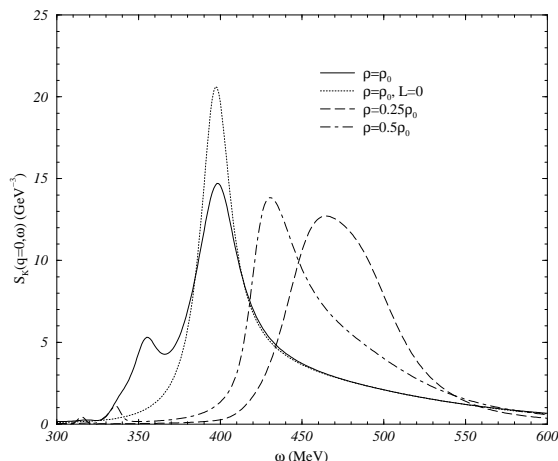


Figure 3.  $K^-$  spectral density for zero momentum using the Jülich  $\bar{K}N$  potential (from [24]).

As an example on the importance of dressing the antikaon, we show in Fig. 2 the spectral function of a  $K^-$  meson of zero momentum obtained with the chiral model of ref. [23] for various densities:  $\rho_0$  (solid line),  $\rho_0/2$  (short-dashed line) and  $\rho_0/4$  (long-dashed line). The upper panel corresponds to a calculation in which the antikaons are dressed selfconsistently but the pions are free. At  $\rho_0/4$  one sees two excitation modes. The left one corresponds to the  $K^-$  pole branch, appearing at an energy smaller than the kaon mass,  $m_K$ , due to the attractive  $\bar{K}N$  amplitude. The peak on the right corresponds to the  $\Lambda(1405)$ -hole excitation mode, which appears around  $m_K$ . As density increases, the  $K^-$  feels an enhanced attraction while the  $\Lambda(1405)$ -hole peak loses strength and dissolves

in the dense nuclear medium. When the dressing of the pion is also incorporated, the effective interaction  $T_{\text{eff}}$  becomes even smoother and the resulting  $K^-$  spectral function is displayed in the bottom panel of Fig. 2. Even at very small densities one can no longer distinguish the  $\Lambda(1405)$ -hole peak from the  $K^-$  pole one. As density increases, the attraction felt by the  $K^-$  is more moderate and the  $K^-$  pole peak appears at higher energies than before. However, more strength is found at very low energies, especially at  $\rho_0$ , due to the particle-hole ( $ph$ ) components of the pionic strength, which couple the  $\bar{K}N$  pair to  $ph\Sigma$  states. It is precisely the opening of the  $\pi\Sigma$  channel, on top of the already opened  $ph\Sigma$  one, which causes a cusp around 400 MeV. The calculation of ref. [24] using the Jülich  $\bar{K}N$  interaction, shown in Fig. 3, obtains qualitatively similar results as those in the upper panel of Fig. 2, where only antikaons are dressed. We notice an additional structure in the spectral function to the left of the quasiparticle peak at energies of the  $\bar{K}$  around 320 – 360 MeV, which is not present when only the  $L = 0$  component of the  $\bar{K}N$  interaction is retained (dotted line). This peak is indicating the physical in-medium excitation of  $\Sigma h$  states with antikaon quantum numbers coming from the  $L = 1, I = 1$  component of the  $\bar{K}N$  interaction.

A non-relativistic antikaon potential can be obtained from the self-energy at the quasiparticle energy via the relation

$$U_K(\vec{q}) = \frac{\Pi_K(\varepsilon_{qp}(\vec{q}), \vec{q}, \rho)}{2m_K}. \quad (6)$$

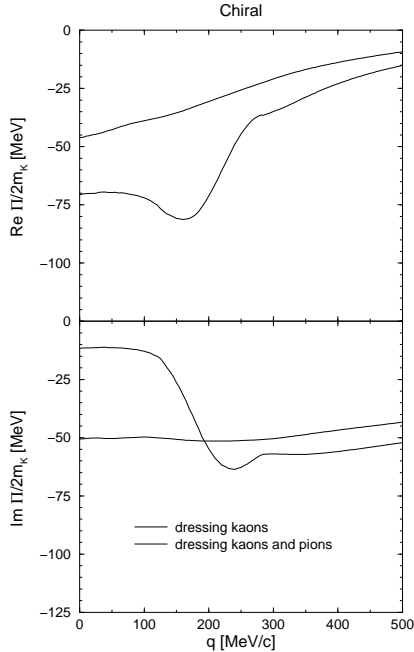


Figure 4. Real and imaginary parts of the  $\bar{K}$  optical potential at  $\rho = \rho_0$  as functions of the antikaon momentum obtained from the chiral model of ref. [23].

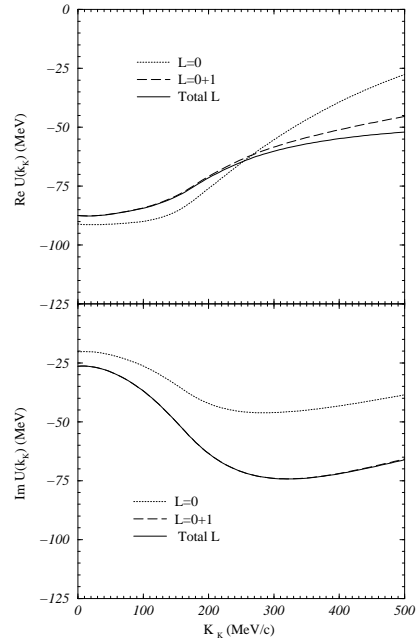


Figure 5. The same as Fig. 4 obtained in ref. [24] using the Jülich  $\bar{K}N$  potential.

The momentum dependence of the potential obtained from the chiral model of ref. [23] at  $\rho = \rho_0$  is shown in Fig. 4 for two approximations, one in which only the antikaons are dressed self-consistently (thin solid lines) and another in which the self-energy of the pions is also included (thick solid line). Note that the antikaon potential obtained when the pions are also dressed has much less structure. This is due in part to the smoother in-medium amplitude, but also to the different quasiparticle energy at which the antikaon self-energy is evaluated. This quasiparticle energy is more attractive when only antikaons are dressed and, hence, the amplitude is explored at lower energy regions, closer to the position of the in-medium  $\Lambda(1405)$  resonance. Results from the model of ref. [24] using the Jülich  $\bar{K}N$  potential are shown in Fig. 5, where the effect of including the higher partial waves can be seen. Already at zero momentum, Fermi motion induces some small contribution of partial waves higher than  $L = 0$ . Clearly, the effect of the higher partial waves increases with increasing  $\bar{K}$  momentum, flattening out the real part of the potential and producing more structure to the imaginary part. At an antikaon momentum of around 500 MeV/c, the inclusion of the higher partial waves practically doubles the size of the antikaon potential with respect to the  $S$ -wave value.

## 5. Kaonic atoms

Since in kaonic atoms the  $K^-$  is bound with a small (atomic) energy, their study requires the knowledge of the antikaon self-energy at  $(q^0, \vec{q}) = (m_K, \vec{0})$ . The density-dependent self-energy obtained with the chiral model has been recently used to study kaonic atoms in the framework of a local density approximation [10], which amounts to replace the nuclear matter density  $\rho$  by the density profile  $\rho(r)$  of the particular nucleus. The results, displayed in Fig. 6, show that both the energy shifts and widths of kaonic atom states agree well with the bulk of experimental data [40]. Recent investigations that respect the low density theorem [41] show that the non-local corrections, coming from the energy and momentum dependence of the potential, from the  $P$ -wave terms of the meson-baryon lagrangian and from Fermi motion, are small and lead to changes in the widths and shifts smaller than the experimental errors.

Reproducing kaonic atom data with the moderately attractive antikaon nucleus potential of  $-45$  MeV obtained from the chiral model [10] is in contrast with the depth of around  $-200$  MeV obtained from a best fit to  $K^-$  atomic data with a phenomenological potential that includes an additional non-linear density dependent term [8]. A clarifying quantitative comparison of kaonic atom results obtained with various  $K^-$ -nucleus potentials can be found in ref. [11]. It is shown there that adding to the chiral potential a phenomenological piece, which is fitted to the data, the  $\chi^2/d.o.f.$  is reduced from 3.8 to 1.6. The resulting potential is slightly more attractive ( $-50$  MeV at  $\rho_0$ ) and the imaginary part is reduced by about a factor 2. The work of ref. [11] reemphasizes that kaonic atoms only explore the antikaon potential at the surface of the nucleus. Therefore, although all models predict attraction for the  $K^-$ -nucleus potential, the precise value of its depth at the center of the nucleus, which has important implications for the occurrence of kaon condensation, is still not known. It is then necessary to gather more data that could help in disentangling the properties of the  $\bar{K}$  meson in the medium. Apart from the valuable information that can be extracted from the production of  $K^-$  in heavy-ion collisions, one



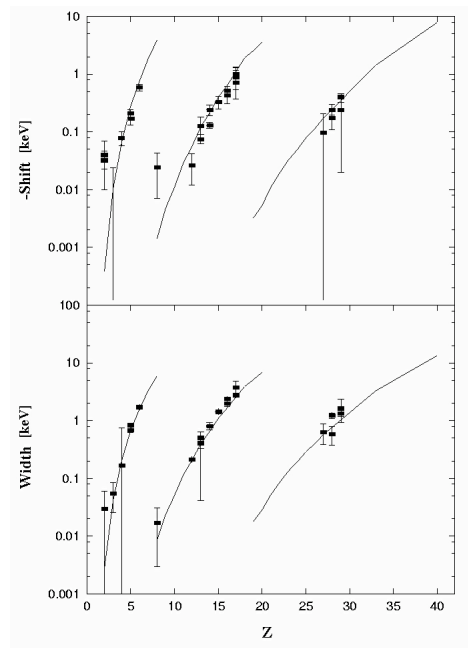


Figure 6. Energy shifts and widths of kaonic atom states (from [10]). The experimental data are taken from the compilation given in [40].

could also study deeply bound kaonic states, which have been predicted to be narrow [10,11,42] and could be measured in  $(K^-, \gamma)$  [10] or  $(K^-, p)$  reactions [43,44].

## Acknowledgments

We would like to acknowledge financial support from the DGICYT (Spain) under contracts PB96-0753, PB98-1247, from the Generalitat de Catalunya under grant SGR2000-24, and from the EU TMR network Eurodaphne contract ERBFMRX-CT98-0169. L.T. acknowledges support from a doctoral fellowship of the Ministerio de Educación y Cultura (Spain).

## REFERENCES

1. D.B. Kaplan and A.E. Nelson, Phys. Lett. B **175**, 57 (1986), *ibid* **179**, 409 (Erratum).
2. G.E. Brown, K. Kubodera, M. Rho, and V. Thorsson, Phys. Lett. B **291**, 355 (1992).
3. H. Fujii, T. Maruyama, T. Muto, and T. Tatsumi, Nucl. Phys. **A597**, 645 (1996).
4. G.Q. Li, C.-H. Lee, and G.E. Brown, Phys. Rev. Lett. **79**, 5214 (1997).
5. P.J. Ellis, R. Knorren, and M. Prakash, Phys. Lett. B **349**, 11 (1995).
6. N.K. Glendenning and J. Schaffner-Bielich, Phys. Rev. Lett. **81**, 4564 (1998).
7. J.A. Pons, S. Reddy, P.J. Ellis, M. Prakash, J.M. Lattimer, Phys. Rev. **C62**, 035803 (2000).
8. E. Friedman, A. Gal, and C.J. Batty, Nucl. Phys. **A579**, 518 (1994).
9. A. Gal, these proceedings.

10. S. Hirenzaki, Y. Okumura, H. Toki, E. Oset, and A. Ramos, Phys. Rev. C **61**, 055205 (2000).
11. A. Baca, C. García-Recio, and J. Nieves, Nucl. Phys. **A673**, 335 (2000).
12. R. Barth et al., Phys. Rev. Lett. **78**, 4007 (1997); F. Laue et al., Phys. Rev. Lett. **82**, 1640 (1999).
13. W. Cassing, E.L. Bratkovskaya, U. Mosel, S. Teis, and A. Sibirtsev, Nucl. Phys. **A614**, 415 (1997); E.L. Bratkovskaya, W. Cassing, and U. Mosel, Nucl. Phys. **A622**, 593 (1997).
14. G.Q. Li, C.-H. Lee, and G.E. Brown, Nucl. Phys. **A625**, 372 (1997).
15. J. Schaffner-Bielich, V. Koch, and M. Effenberg, Nucl. Phys. **A669**, 153 (2000).
16. C.-H. Lee, Phys. Reports **275**, 255 (1996) and references therein.
17. G. Mao, P. Papazoglou, S. Hofmann, S. Schramm, H. Stöcker, and W. Greiner, Phys. Rev. C **59**, 3381 (1999).
18. J. Schaffner-Bielich, I.N. Mishustin, and J. Bondorf, Nucl. Phys. **A625**, 325 (1997).
19. M. Alberg, E.M. Henley, and L. Wilets, Ann. Phys. (N.Y.) **96**, 43 (1976).
20. V. Koch, Phys. Lett. B **337**, 7 (1994).
21. T. Waas, N. Kaiser, and W. Weise, Phys. Lett. B **365**, 12 (1996); T. Waas and W. Weise, Nucl. Phys. **A625**, 287 (1997).
22. M. Lutz, Phys. Lett. B **426**, 12 (1998).
23. A. Ramos and E. Oset, Nucl. Phys. **A671**, 481 (2000).
24. L. Tolós, A. Ramos, A. Polls, and T.T.S. Kuo, Nucl. Phys. **A**, in print, nucl-th/0007042.
25. E. Oset and A. Ramos, Nucl. Phys. **A635**, 99 (1998).
26. A. Müller-Groeling, K. Holinde, and J. Speth, Nucl. Phys. **A513**, 557 (1990).
27. N. Kaiser, P.B. Siegel and W. Weise, Nucl. Phys. **A594**, 325 (1995).
28. J. A. Oller and E. Oset, Nucl. Phys. **A620**, 438 (1997); erratum Nucl. Phys. **A624**, 407 (1999).
29. J. A. Oller, E. Oset, and J. R. Peláez, Phys. Rev. Lett. **80**, 3452 (1998); Phys. Rev. D **59**, 074001 (1999); erratum Phys. Rev. D **60**, 099906 (1999).
30. J.A. Oller and U.G. Meissner, hep-ph/0011146.
31. D.N. Tovee et al., Nucl. Phys. **B33**, 493 (1971).
32. R.J. Nowak et al., Nucl. Phys. **B139**, 61 (1978).
33. A.D. Martin, Nuc. Phys. **B179**, 33 (1981).
34. S.S. Kamalov, E. Oset, and A. Ramos, Nucl. Phys. **A**, in print. nucl-th/0010054.
35. R. Chand and R. H. Dalitz, Ann. Phys. (N.Y.) **20**, 1 (1962).
36. G. Toker, A. Gal, and J. M. Eisenberg, Nucl. Phys. **A362**, 405 (1982).
37. M. Torres, R. H. Dalitz and A. Deloff, Phys. Lett. **B174**, 213 (1986).
38. A. Deloff, Phys. Rev. **C61**, 024004 (2000).
39. J. Caro, N. Kaiser, S. Wetzell, and W. Weise, Nucl. Phys. **A672**, 249 (2000).
40. C. J. Batty, E. Friedman, and A. Gal, Phys. Rep. **287**, 385 (1997).
41. C. García-Recio, E. Oset, A. Ramos, and J. Nieves, nucl-th/0012075.
42. E. Friedman and A. Gal, Phys. Lett. B **459**, 43 (1999).
43. E. Friedman and A. Gal, Nucl. Phys. **A658**, 345 (1999).
44. T. Kishimoto, Phys. Rev. Lett. **83**, 4701 (1999).